Materials & Design 210 (2021) 110031

Contents lists available at ScienceDirect

Materials & Design

journal homepage: www.elsevier.com/locate/matdes

Quadramode materials: Their design method and wave property

Yu Wei, Xiaoning Liu, Gengkai Hu *

School of Aerospace Engineering, Beijing Institute of Technology, Beijing 100081, China

HIGHLIGHTS

- Wave characteristics of different quadramode materials according to material symmetry are systematically investigated.
- A quadramode material supporting any combination of two shear stresses is proposed and validated for the first time.
- An out-of-plane shear (SH) wave polarizer is constructed with the proposed quadramode material.

GRAPHICAL ABSTRACT

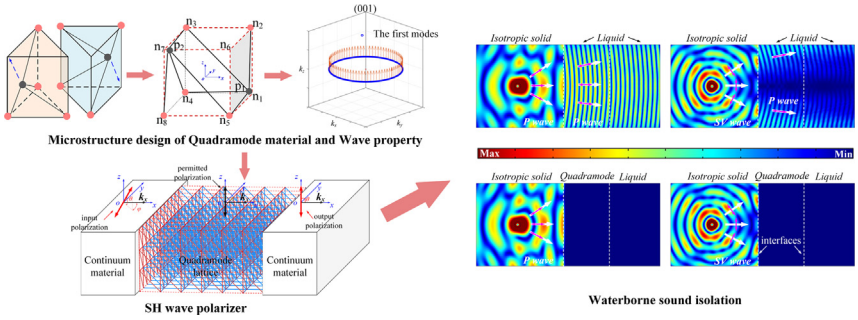

ARTICLE INFO

Article history:
Received 28 May 2021
Revised 19 July 2021
Accepted 5 August 2021
Available online 6 August 2021

Keywords:
Extremal material
Quadramode
Microstructure design
Elastic wave
Waterborne sound isolation

ABSTRACT

Extremal materials with certain vanishing eigenvalues of their elastic matrix are able to manipulate elastic wave with their extremal static property, the devices designed with such materials can work in a broad frequency band, which is highly demanded in low frequency applications. A type of extremal materials with four zero eigenvalues called quadramode (QM) materials is the subject of this investigation. Wave properties of different QM materials, particularly their capacity on shaping *iso*-frequency curves, are firstly examined with homogeneous models. A three-dimensional QM material is then designed using a truss lattice model. The designed lattice is validated through comparison between the homogeneous and discrete models on their prediction on *iso*-frequency curves and polarizations. An out-of-plane shear (SH) wave polarizer is proposed with the designed QM material, it can effectively prevent the mode conversion at interface with fluids. This unique property is further explored for waterborne sound isolation, a prototype of this polarizer is also proposed and demonstrated through numerical simulation. This study paves the way for exploring the exotic wave properties of QM extremal materials, and opens a new route to control low frequency elastic wave.

1. Introduction

Responses of linear Cauchy elastic materials are characterized by Hooke's law with elastic stiffness tensors depending intimately on their microstructures. Classification of materials according to the property of their elastic tensors dated back quite early, e.g., the symmetry of material microstructure reduces significantly the number of material constants, from 21 for a general elastic material to 2 for an isotropic material [1]. More recently, emergence of elastic metamaterials extends available range of elastic tensor, e.g., from positive elastic moduli to negative ones [2–4], or relaxes constraints on minor symmetry [5–7] and major symmetry [8] of elastic tensor. These extensions enable continuum mechanics to characterize more complex phenomena surged from interaction between loading and microstructure.

Another interesting classification of materials was proposed by Milton and Cherkaev [9] (see also [10]), they classified materials according to the number of zero eigenvalues of elasticity matrix: *unimode* (UM) if there is one zero eigenvalue, successively *bimode*

* Corresponding author.
E-mail address: hugeng@bit.edu.cn (G. Hu).

https://doi.org/10.1016/j.matdes.2021.110031
0264-1275/

(BM), *trimode* (TM), *quadramode* (QM) and *pentamode* (PM) if there are five. The eigenvectors corresponding to zero eigenvalues represent *mechanisms* of materials, i.e., zero energy modes. Materials with zero eigenvalues of elasticity matrix are not stable, there are inherent *mechanisms* embedded in the materials. These materials are referred to as extremal materials in the following [9]. Due to the embedded *mechanisms*, extremal materials may have very special mechanical properties, e.g., very hard in some stress states and very soft for the others, useful for particular engineering applications. According to this classification, liquids are special kind of PM materials, supporting only hydrostatic stress and being soft for any other stress states. We can approximately realize PM materials with solids [11,12], which can mimic wave properties of liquids. The materials and devices made of solid PM materials are intrinsically broadband and are of great value in underwater acoustic wave control [13].

Extremal materials have been recognized as a rapid development recently, primarily focusing on PM materials. Norris [14] demonstrated that acoustic cloak can be designed with PM materials, few years later the first solid PM materials was fabricated by Kadic et al. [11] based on the diamond lattice proposed by Milton and Cherkaev [9], these works refueled the research on PM materials. Layman et al. [15] proposed an oblique honeycomb lattice to design PM materials with anisotropic properties. Norris [16] examined the condition of lattice networks to realize PM materials. Based on honeycomb lattice, Chen et al. [12] proposed a new microstructural configuration of PM materials, which can achieve a large anisotropic ratio in moduli. A microstructure prototype of PM material with anisotropic density is also proposed [17]. More recently, based on topology optimization techniques, many novel microstructures of PM materials can be put forward [18,19]. With the development of design and fabrication methods for PM materials, many functional devices have been proposed, such as static mechanical cloak [20], underwater sound cloak [13], polarization tailoring [21], even seismic wave alleviation [22].

Apart from PM materials, only few work was devoted to the study on other modes of extremal materials. There are some possible examples of UM materials in both two- [9,23–25] and three-dimension [9,26]. From these examples, as well as PM material design, we see that these extremal materials are constructed by designing the necessary *mechanism* in periodic pin-jointed trusses or a composite, quantitative relationship between designed structure and its elastic property is also necessary and not provided. Therefore, there is still an urgent need to study this kind of extremal materials and explore their possible engineering applications.

In this paper, we will examine systematically QM materials with periodic pin-jointed truss model. Classification of QM materials based on material symmetry and their corresponding wave characteristics are explained in Section 2. A QM material with transversely isotropic symmetry is described in detail, and a design method is proposed and validated by both discrete and homogenized models, this will be detailed in Section 3. Section 4 explores some applications of the QM material. Elastic wave refractions between QM and ordinary isotropic solid materials as well as liquids are also considered, an application of waterborne sound isolation is investigated. In the end, some conclusions will be drawn.

2. Wave property of quadramode materials

2.1. Classification of QM materials

The elastic tensor of QM materials, in form of Kelvin's decomposition, is expressed by $\mathbf{C} = K_1\mathbf{S}_1 \otimes \mathbf{S}_1 + K_2\mathbf{S}_2 \otimes \mathbf{S}_2$, with $\mathbf{S}_i (i = 1, 2)$ being a 2nd order symmetric tensor. $K_i (i = 1, 2)$ is the non-zero eigenvalues of the elastic matrix, implying that the QM material is stiff to any stress in the subspace spanned by $\mathbf{S}_1$ and $\mathbf{S}_2$. For convenience, the elastic tensor is also written as $\mathbf{C} = \sum \mathbf{S}_i \otimes \mathbf{S}_i$, where K_i is absorbed in $\mathbf{S}_i$. In the Voigt's notation, $\mathbf{C}$ will be written as a 6×6 elastic matrix and $\mathbf{S}$ the 6×1 stress vector, respectively. QM materials are completely determined by the two non-zero eigenvalues (K_1 and K_2) and its characteristic stresses ($\mathbf{S}_1$ and $\mathbf{S}_2$). To check if a material is QM, it suffices to evaluate *rank* ($\mathbf{C}$) = 2. However, there are a large number of possible forms of the elastic matrix to be QM. In the following, we will discuss QM materials from material symmetry.

Firstly, we consider isotropic materials. The elastic matrix of isotropic materials has only two independent components C_{11} and C_{12} as follows

$$\mathbf{C} = \begin{bmatrix} C_{11} & C_{12} & C_{12} & 0 & 0 & 0 \\ C_{12} & C_{11} & C_{12} & 0 & 0 & 0 \\ C_{12} & C_{12} & C_{11} & 0 & 0 & 0 \\ 0 & 0 & 0 & (C_{11}-C_{12})/2 & 0 & 0 \\ 0 & 0 & 0 & 0 & (C_{11}-C_{12})/2 & 0 \\ 0 & 0 & 0 & 0 & 0 & (C_{11}-C_{12})/2 \end{bmatrix}. \tag{1}$$

Now, let's consider the case that $C_{11} \neq C_{12}$, it's obvious that the *rank* ($\mathbf{C}$) is equal to 6, i.e. they are null mode materials. While, if we consider the case that $C_{11} = C_{12}$, there must be only one non-zero eigenvalue for such elastic matrix, indicating they are PM materials. As a consequence, a QM material cannot be isotropic.

Secondly, we consider materials with transversely isotropic symmetry and its elastic matrix has the following form with five independent components

$$\mathbf{C} = \begin{bmatrix} C_{11} & C_{12} & C_{13} & 0 & 0 & 0 \\ C_{12} & C_{11} & C_{13} & 0 & 0 & 0 \\ C_{13} & C_{13} & C_{33} & 0 & 0 & 0 \\ 0 & 0 & 0 & C_{44} & 0 & 0 \\ 0 & 0 & 0 & 0 & C_{44} & 0 \\ 0 & 0 & 0 & 0 & 0 & (C_{11}-C_{12})/2 \end{bmatrix}. \tag{2}$$

Obviously, there are many kinds of QM materials with transverse isotropy. Here we will examine an interesting example, $C_{11} = C_{33} = C_{12} = C_{13} = 0$ and $C_{44} = 1$ (here 1 means the component has the same magnitude and non-zero value, the same for characteristic stress), which supports only stress states linearly combined by $\mathbf{S}_1 = [0, 0, 0, 1, 0, 0]^T$ and $\mathbf{S}_2 = [0, 0, 0, 0, 1, 0]^T$. More specifically, this QM material can support any stress consisting of pure shear stress $\mathbf{S}_{23}$ and $\mathbf{S}_{13}$.

The *iso*-frequency surfaces (IFS) of this type of QM material are shown in Fig. 1, there are only two IFS in wave vector space, different from three for an ordinary solid material. The reason for this will be clarified in Section 2.2. Fig. 1 (a) and (b) show the shape of the IFS of the first and the second mode, respectively, the first is a sphere and the second is two parallel planes. Fig. 1(c) and (e) illustrate the *iso*-frequency curves (IFC) sliced on the (100) and (001) planes, respectively. The orange and purple arrows represent the polarization of the first and the second mode, respectively. According to the IFC and their polarization, the material behaves as an isotropic PM material on (001) plane which can support only one wave mode with polarization always perpendicular to the wave vector. This character is very different from a pure isotropic PM material for which the single wave mode is polarized in parallel to the wave vector.

Thirdly, we consider orthotropic materials, and their elastic matrix has the following form with nine independent components:

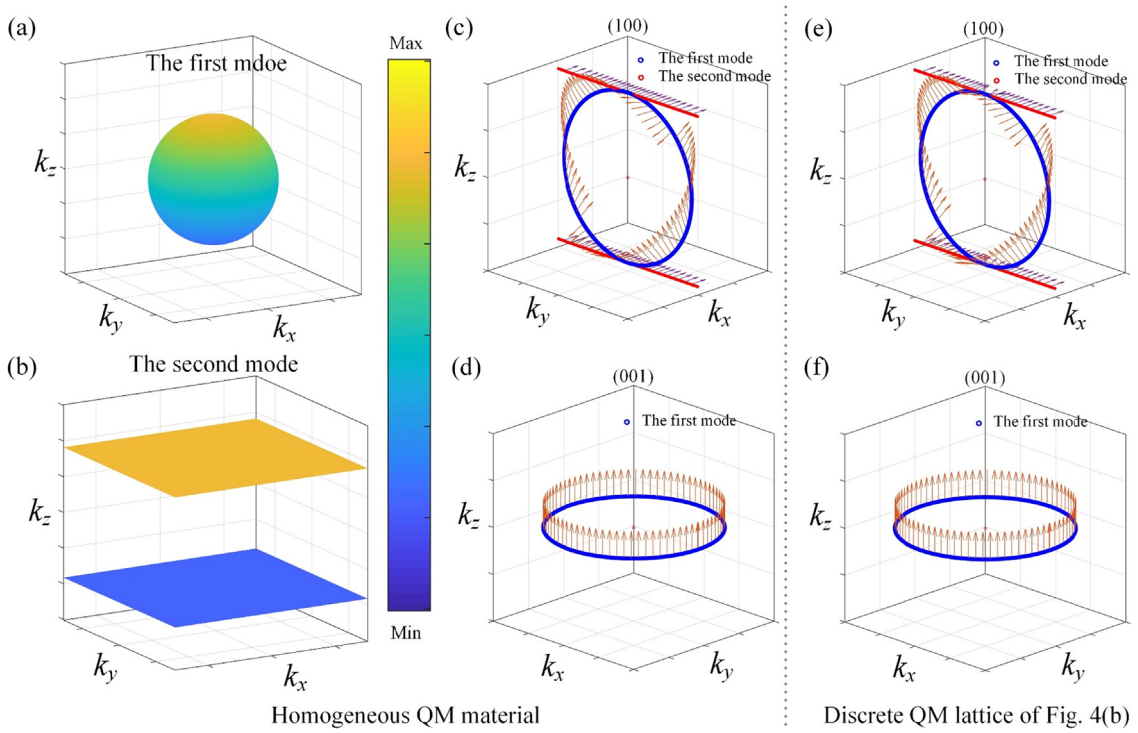

Fig. 1. IFS of a QM material with $\mathbf{S}_1 = [0, 0, 0, 1, 0, 0]^T$ and $\mathbf{S}_2 = [0, 0, 0, 0, 1, 0]^T$. (a)-(d) for homogeneous QM: (a) the first mode; (b) the second mode; IFC and the polarization on (c) (100) and (d) (001) plane; (e)-(f) same as (c)-(d) but the homogeneous QM materials is replaced by its discrete QM lattice.

$$\mathbf{C} = \begin{bmatrix} C_{11} & C_{12} & C_{13} & 0 & 0 & 0 \\ C_{12} & C_{22} & C_{23} & 0 & 0 & 0 \\ C_{13} & C_{23} & C_{33} & 0 & 0 & 0 \\ 0 & 0 & 0 & C_{44} & 0 & 0 \\ 0 & 0 & 0 & 0 & C_{55} & 0 \\ 0 & 0 & 0 & 0 & 0 & C_{66} \end{bmatrix}. \tag{3}$$

With the condition for QM, we can also find many combinations of these components rendering a QM material with orthotropic symmetry. Here is given one of such examples with $C_{11} = C_{22} = C_{33} = C_{12} = C_{13} = C_{23} = C_{66} = 1$ and $C_{44} = C_{55} = 0$, corresponding to the two characteristic stresses $\mathbf{S}_1 = [1, 1, 1, 0, 0, 0]^T$ and $\mathbf{S}_2 = [0, 0, 0, 0, 0, 1]^T$. This QM material is stiff to any stress in the subspace spanned by a pure shear stress and hydrostatic pressure.

The IFS of this QM material are shown in Fig. 2. In the figure, (a) and (b) reveal the characteristic of IFS for the first and the second mode, respectively. In the first mode, the IFS is a closed surface, its skeleton is composed of two orthogonal circles (specified by black solid lines) and its equator is made of a square (specified by blue solid/dashed lines). And the second consists of intersecting hollow tubes. The IFC on (100) and (001) planes are also shown in Fig. 2 (c) and (d), and their polarization indicated by orange (the first mode) and purple (the second mode) arrows, respectively. Interestingly, on the (001) plane as shown in Fig. 2(d), the IFC are composed of segmented straight lines, closed square for the first mode and open parallel lines intersected with the square for the second mode.

Finally, we consider monoclinic materials (eg. *xoy*-plane), their elastic matrix has the following form with thirteen independent components.

$$\mathbf{C} = \begin{bmatrix} C_{11} & C_{12} & C_{13} & 0 & 0 & C_{16} \\ C_{12} & C_{22} & C_{23} & 0 & 0 & C_{26} \\ C_{13} & C_{23} & C_{33} & 0 & 0 & C_{36} \\ 0 & 0 & 0 & C_{44} & C_{45} & 0 \\ 0 & 0 & 0 & C_{45} & C_{55} & 0 \\ C_{16} & C_{26} & C_{36} & 0 & 0 & C_{66} \end{bmatrix}. \tag{4}$$

Obviously, there are many combinations of the components to form a monoclinic QM material. Let us consider the following example where all the components in Eq. (4) are set to be 1, corresponding to the characteristic stresses $\mathbf{S}_1 = [1, 1, 1, 0, 0, 1]^T$ and $\mathbf{S}_2 = [0, 0, 0, 1, 1, 0]^T$.

The IFS of this QM material are shown in Fig. 3. As illustrated in Fig. 3 (a) and (b), the IFS are a hollow tube for the first mode and four non-intersect V-shaped planes for the second mode. Fig. 3(c) and (d) show respectively the IFC on the planes (100) and (001), and their polarizations indicated respectively by orange and purple arrows. It's worth noting that the polarizations of both the first and the second mode in Fig. 3(c) are neither parallel nor perpendicular to the crystal plane, which means when considering the wave characteristics on these crystal planes, it cannot be simplified as a two dimensional plane problem. In addition, the IFC on the (001) plane are two parallel lines, indicating that the energy of bulk wave can only propagate within the plane perpendicular to the IFC.

2.2. Number of IFS for extremal materials

It is shown through concrete examples in the previous section that QM materials possess only two modes, distinct from three for ordinary solids. In this section, we will establish the connection between number of IFS (or IFC) and different modes of extremal

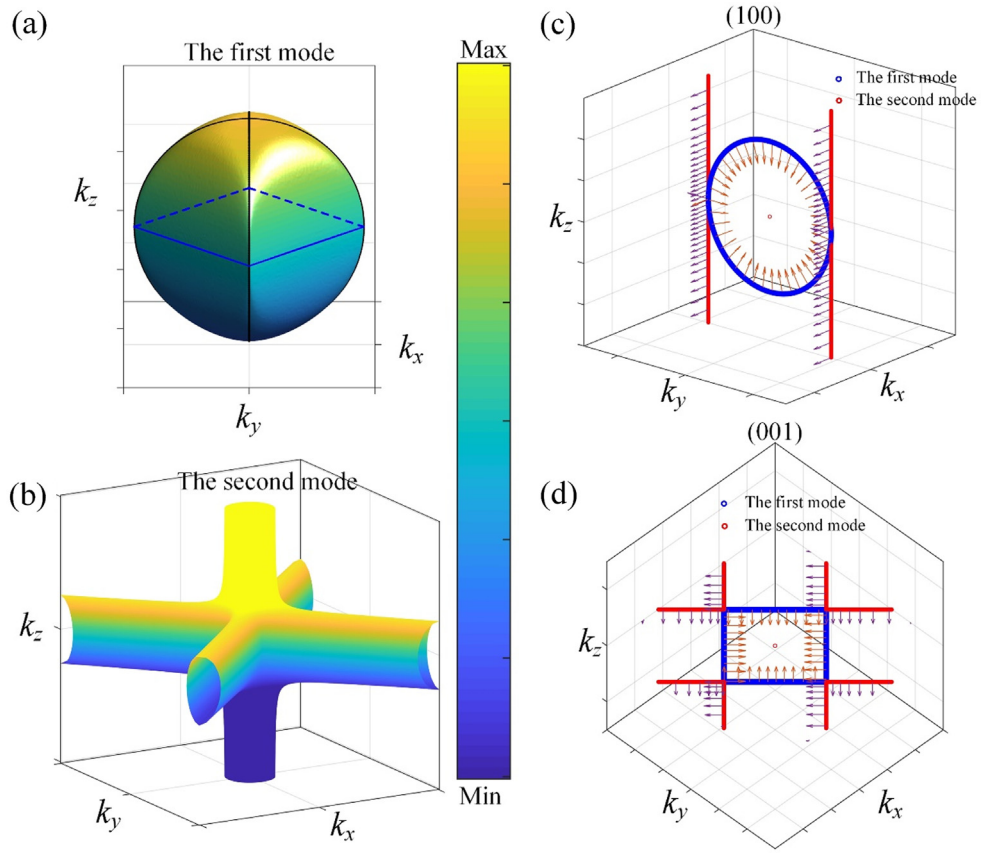

Fig. 2. The IFS of a QM material with $\mathbf{S}_1 = [1, 1, 1, 0, 0, 0]^T$ and $\mathbf{S}_2 = [0, 0, 0, 0, 0, 1]^T$. (a) the first mode; (b) the second mode; IFC and its polarization on (c) (100) and (d) (001) planes.

materials. For a plane harmonic solution $u_i = A_i \exp[\mathrm{i}(k_j x_j - \omega t)]$ (i is complex number) propagating in an elastic material of elastic tensor C_{iklm}, the Christoffel's equation is given by [27]

$$(\Gamma_{im} - \rho c^2 \delta_{im}) u_m = 0. \tag{5}$$

where acoustic tensor $\Gamma_{im} = C_{iklm} n_k n_l$, $\boldsymbol{n}$ is the direction cosine of the wave vector, and c is the phase velocity. Let $\zeta = \rho c^2$, the characteristic equation then can be expanded as

$$\zeta^3 - \mathrm{tr}(\boldsymbol{\Gamma})\zeta^2 + \mathrm{tr}(\boldsymbol{\Gamma}^*)\zeta - \det(\boldsymbol{\Gamma}) = 0. \tag{6}$$

By defining the function $\boldsymbol{N}$, the acoustic tensor can be written as:

$$\boldsymbol{\Gamma} = \boldsymbol{N}\boldsymbol{C}\boldsymbol{N}^T, \tag{7}$$

where $\boldsymbol{N}$ is defined by

$$N = \begin{bmatrix} n_1 & 0 & 0 & 0 & n_3 & n_2 \\ 0 & n_2 & 0 & n_3 & 0 & n_1 \\ 0 & 0 & n_3 & n_2 & n_1 & 0 \end{bmatrix}, \tag{8}$$

For a general solid material, the Eq. (6) always has three non-zero solutions, i.e. three phase velocities. While, for QM materials, there are only two non-zero solutions at most. To be more specific, we have

$$rank(\boldsymbol{\Gamma}) = rank\left(\boldsymbol{N}\boldsymbol{C}\boldsymbol{N}^T\right) \le \min\left(rank(\boldsymbol{N}), rank(\boldsymbol{C}), rank\left(\boldsymbol{N}^T\right)\right) \tag{9}$$

where $rank(\boldsymbol{N}) = rank\left(\boldsymbol{N}^T\right) = 3$, $rank(\boldsymbol{C}) = 2$. Then we can see that the *rank* of Γ is always no more then 2, i.e. $rank(\boldsymbol{\Gamma}) \le m_\Gamma - 1$, where m_Γ is the order of symmetric matrix Γ. Through some linear algebra, it can be shown that for any QM material and any given direction of $\boldsymbol{n}$, $\det(\boldsymbol{\Gamma})$ is always equal to zero and $\mathrm{tr}(\boldsymbol{\Gamma}^*)$ might be non-zero. Then the Eq. (6) can be rewritten as

$$\left[\zeta^2 - \mathrm{tr}(\boldsymbol{\Gamma})\zeta + \mathrm{tr}(\boldsymbol{\Gamma}^*)\right]\zeta = 0. \tag{10}$$

In this way, for QM materials, the Eq. (6) can only find two non-zero solutions at most, that is why there are only two IFS noticed in the previous section.

Similarly, it can be shown $rank(\boldsymbol{\Gamma}) \le m_\Gamma - 2$ for a given PM material, indicating that the $\det(\boldsymbol{\Gamma})$ and $\mathrm{tr}(\boldsymbol{\Gamma}^*)$ are both equal to zero for any PM material and any direction of $\boldsymbol{n}$. So for PM materials, there is only one non-zero solution at most.

3. Design method of quadramode materials

3.1. Design principle

As proposed by Milton and Cherkaev [9], all three-dimensional materials (including extremal materials) can be assembled from appropriate PM materials. Following their idea, we will design the QM materials analyzed in the previous section. In the following, we will homogenize PM/QM lattice based on pin-joint truss model, in which all the rods are only subjected to axial loads and the effect of 3D stress distribution is neglected. Therefore, the proposed construction methodology only works for low density regime.

Firstly, we select a PM lattice as shown in Fig. 4(a), which contains 5 nodes and 4 rods. Maxwell's rule indicates that there are five independent inextensional *mechanisms* in such lattice [28–30]. Moreover, the characteristic stress tensors of the lattice can

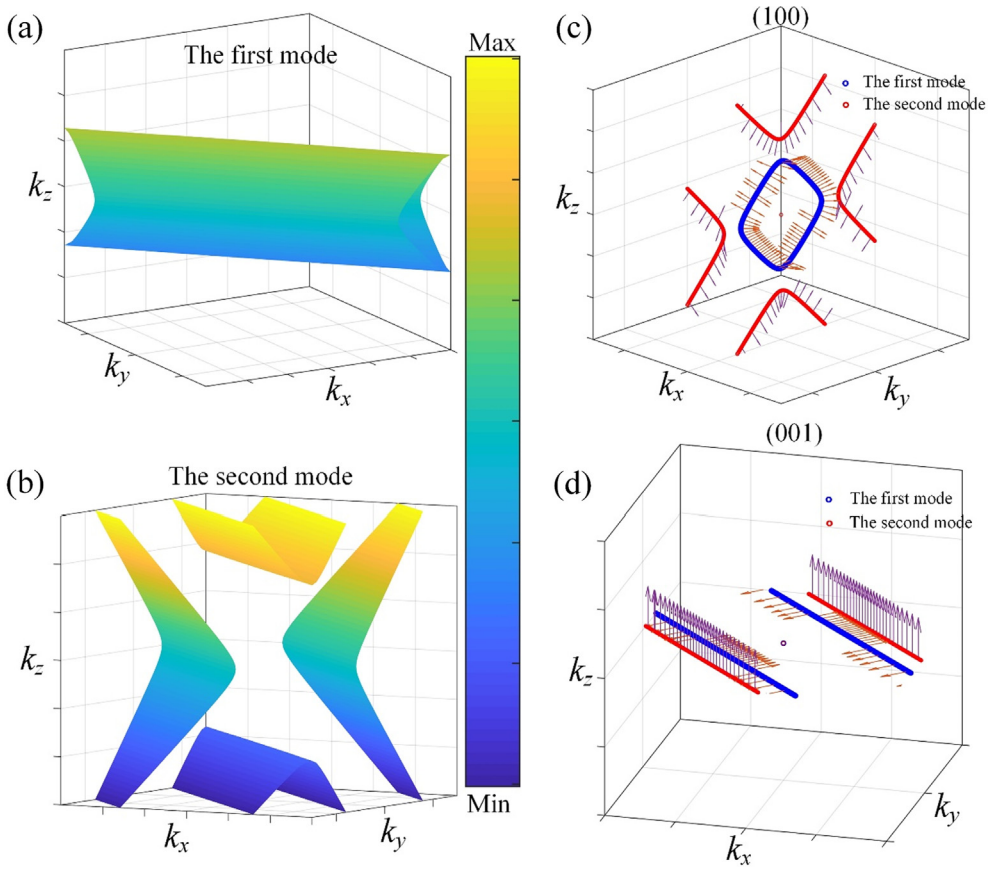

Fig. 3. The IFS of a QM material with the characteristic stresses $\mathbf{S}_1 = [1, 1, 1, 0, 0, 1]^T$ and $\mathbf{S}_2 = [0, 0, 0, 1, 1, 0]^T$. (a) the first mode; (b) the second mode; IFC and its polarization on (c) (100) and (d) (001) planes.

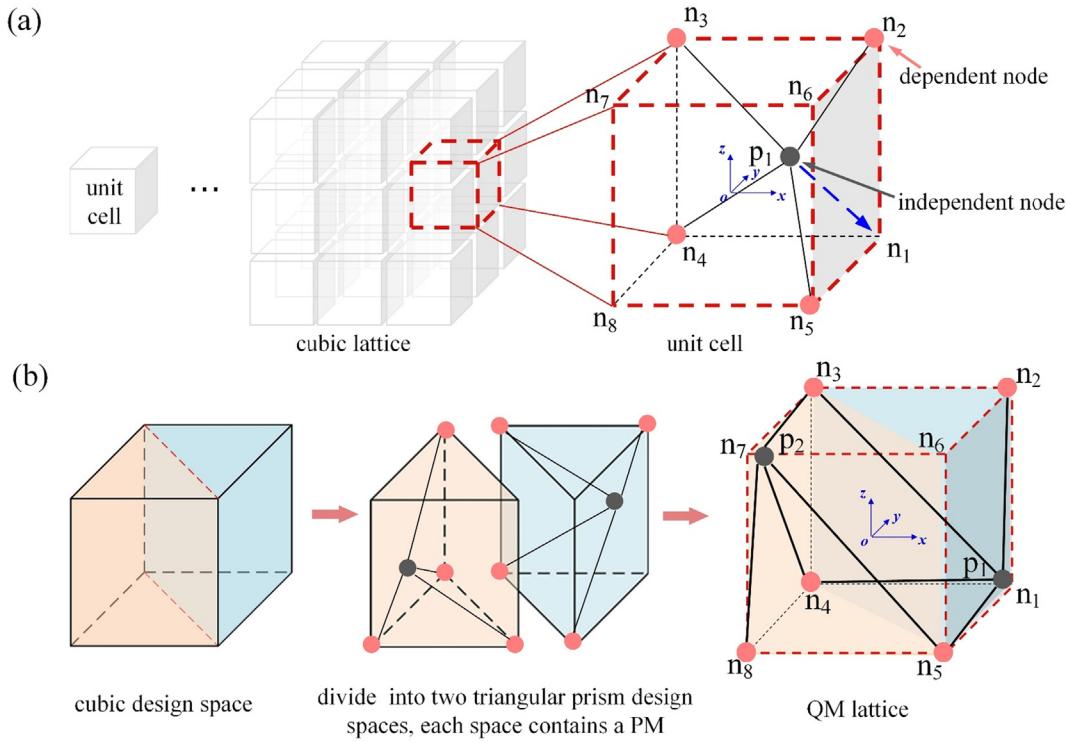

Fig. 4. Design principle for QM lattice. (a) PM lattice used to build QM lattice, it contains four light red dependent nodes at the cubic boundary and one dark gray independent node inside; (b) two PM lattices are assembled in one cubic space to build the desired QM lattice.

be obtained by adjusting the position of the internal joint P_1. The advantage of choosing the lattice of Fig. 4(a) is that only four non-coplanar nodes on the boundary of a cube with one internal node are needed to build up a PM lattice. Therefore, only one triangular prism space is enough to provide such a set of nodes for a PM lattice. While there are two triangular prisms in one cube, so two such PM lattices can be constructed in one cube to form a QM lattice with desired function as shown in Fig. 4(b). Meanwhile, it's worth noting that only when the characteristic stresses of two PM are orthogonal to each other, the design principle will be feasible.

To be more specific, in the following we will design a QM material supporting an arbitrary stress consisting of pure shear stresses τ_{yz} and τ_{xz}, which was examined in details in Section 2. For the PM lattice shown in Fig. 4(a), the equivalent property can be obtained by the homogenization method proposed by Norris [16]. However for a QM lattice built up with two PM lattices, numerical method with Cauchy-Born boundary condition on the unit cell has to be utilized to evaluate its effective property [31].

In the computation, we set the lattice constant equal to 2, the Young's modulus, the cross-sectional area and density of each rod are respectively equal to 1. Then, the practical component of elastic matrix is proportional to its corresponding actual one, as noted by Hutchinson and Fleck [31]. It is found that when the joint P_1 in Fig. 4(a) gradually approaches the boundary node n_1 from the inside, the overall lattice will approach an ideal PM lattice supporting only a pure shear stress τ_{xz}. When the coordinates of the joint are $P_1 = [0.995, 0.995, -0.995]^{\mathrm{T}}$ in the Cartesian coordinate system with the center of the cube as shown in Fig. 4(a), the homogenized elastic matrix of the lattice is evaluated as

$$C_{PM} = \begin{bmatrix} 0 & 0 & 0 & 0 & 0.0001 & 0 \\ 0 & 0 & 0 & 0 & 0.0001 & 0 \\ 0 & 0 & 0 & 0 & 0.0001 & 0 \\ 0 & 0 & 0 & 0 & 0 & 0 \\ 0.0001 & 0.0001 & 0.0001 & 0 & 0.0521 & 0 \\ 0 & 0 & 0 & 0 & 0 & 0 \end{bmatrix}. \tag{11}$$

with the eigenvalues $\{\lambda_{PM}\} = \{0.0521, 0, 0, 0, 0, 0\}$, and the eigenvector of the non-zero eigenvalue is $\boldsymbol{x}_{PM} = [0.0019, 0.0019, 0.0019, 0, 1, 0]^T$. The overall lattice can be idealized as an ideal PM material with only characteristic stress τ_{xz}. In the same way, when the node n_2 moves to node n_8, and the internal joint P_2 approaches the node n_7, a new PM lattice supporting only a pure shear stress τ_{yz} is constructed.

Then, we combine the obtained two PM lattices together in the way as shown in Fig. 4(b) to build up the desired QM lattice. The two PM lattices are connected with the nodes n_3, n_4 and n_5 to become a whole, i.e. they are no longer two unrelated PM lattices. The homogeneous elastic matrix $\mathbf{C}_{\mathrm{QM}}$ of this QM lattice is derived as

$$C_{QM} = \begin{bmatrix} 0 & 0 & 0 & 0.0001 & 0.0001 & 0 \\ 0 & 0 & 0 & 0.0001 & 0.0001 & 0 \\ 0 & 0 & 0 & 0.0001 & 0.0001 & 0 \\ 0.0001 & 0.0001 & 0.0001 & 0.0521 & -0.0001 & 0 \\ 0.0001 & 0.0001 & 0.0001 & -0.0001 & 0.0521 & 0 \\ 0 & 0 & 0 & 0 & 0 & 0 \end{bmatrix} \tag{12}$$

with the eigenvalues of the elastic matrix $\{\lambda_{QM}\} = \{0.0522, 0.0520, 0, 0, 0, 0\}$, and $\boldsymbol{x}_{QM_1} = [0, 0, 0, -0.7071, 0.7071, 0]^T$ and $\boldsymbol{x}_{QM_2} = [0.0027, 0.0027, 0.0027, 0.7071, 0.7071, 0]^T$ are the eigenvectors of the two non-zero eigenvalues, respectively. It can be found that the maximum components in either elastic matrix $\mathbf{C}_{\mathrm{QM}}$ or eigenvectors are two orders of magnitude larger than the second largest components. Therefore, the built lattice can be idealized as a QM material supporting an arbitrary stress consisting of the pure shear stress τ_{yz} and τ_{xz}.

As far as practical realization of the proposed quadramode materials, benefiting from the development of modern dip-in three-dimensional DLW optical lithography, the extremal material can be fabricated feasibly, from micro-scale [11,20] to macro-scale [13,21,32–34]. There are usually two techniques to approximate an ideal pin-joint: introducing soft materials in the connection regions [33] or using a finite connection (or overlap) [11,35]. Both indicate that the bulk modulus of an isotropic PM lattice (only support hydrostatic pressure) can be easily made 10^3 time larger than shear modulus by adjusting the distribution of soft materials or the local widths of the connections, in these cases the behavior of the connection is very close to the ideal pin-joint. An active method may provide a new dimension to tailor material microstructure, it is also interesting to explore its possibility for QM design.

3.2. Numerical validation

The dispersion relation of a homogenous QM material can be obtained by calculating the Christoffel's equation with its effective elastic matrix. While for the periodic discrete lattice, the eigenvalue problem of the dynamical matrix will be applied to derive the dispersion relation [36,37]. For a given pin-joint linkage, we can always write out its kinematic equations and equilibrium equation, which in a matrix form read [38]:

$$\boldsymbol{Bd} = \boldsymbol{e}, \tag{13}$$

and

$$\boldsymbol{At} = \boldsymbol{f}, \tag{14}$$

where $\boldsymbol{B}$ is the kinematic matrix, $\boldsymbol{d}$ is the displacement of joints, $\boldsymbol{e}$ is the elongation of rods, $\boldsymbol{A}$ is the equilibrium matrix and $\boldsymbol{A} = \boldsymbol{B}^{\mathrm{T}}$, $\boldsymbol{t}$ is the tension of rods and $\boldsymbol{f}$ is the force of joints. In a pin-jointed lattice, the rod and pin-joint can be considered as 'mass-and-spring' frames [30], and each bond is characterized by Hooke's law spring. Consider spring constant as a diagonal constant matrix $\boldsymbol{k}_b$, then the elastic energy of the lattice is defined as

$$E_p = \frac{1}{2}\boldsymbol{e}^T\boldsymbol{k}_b\boldsymbol{e} = \frac{1}{2}\boldsymbol{d}^T\mathcal{K}\boldsymbol{d}, \tag{15}$$

where

$$\mathcal{K} = \boldsymbol{A}\boldsymbol{k}_b\boldsymbol{A}^T, \tag{16}$$

is the stiffness matrix of the considered lattice. Assume that all mass points have a constant mass m, then the kinetic energy of the lattice is written as

$$E_k = \frac{1}{2}m\dot{\boldsymbol{d}}^T\dot{\boldsymbol{d}}, \tag{17}$$

where $\dot{\boldsymbol{d}}$ is the velocity vector. The normal modes are eigenvectors of the dynamical matrix $\boldsymbol{D} = \mathcal{K}/m$. In order to derive the dispersion relation, we need to evaluate the problem in frequency domain in the first Brillouin zone, implying that

$$\mathcal{K}(\boldsymbol{k}) = \boldsymbol{A}(\boldsymbol{k})\boldsymbol{k}_b\boldsymbol{A}^{\dagger}(\boldsymbol{k}) = m\boldsymbol{D}(\boldsymbol{k}), \tag{18}$$

To obtain the dynamical matrix in periodic pin-jointed structures, the Bloch's theorem is applied to the original kinematic and equilibrium matrices of the unit cell [31,39]. In the primitive unit cell of the QM periodic lattice, we define a direct lattice translation vector $\boldsymbol{x} = x_i\boldsymbol{a}_i$, where x_i is any set of integer values and $\boldsymbol{a}_i$ is

the direct translational basis. And introducing the joint basis $\boldsymbol{j}_k$ ($k = 1, 2, \ldots, J$) for J joints in order to define the location of the independent joints of the unit cell. Thus, we have

$$\boldsymbol{p}_k = \boldsymbol{j}_k + \boldsymbol{x} = \boldsymbol{j}_k + x_i \boldsymbol{a}_i, \tag{19}$$

where $\boldsymbol{p}_k$ is the direct lattice position vectors of all joints $\boldsymbol{j}_k$. Next, we assume that the 3D joint displacement is complex, $\boldsymbol{d}(\boldsymbol{p}_k, \boldsymbol{k}) \in \mathbb{C}^3$, which is defined over the entire lattice using Bloch's theorem for the joint displacement field. Then, Bloch' theorem gives:

$$\boldsymbol{d}(\boldsymbol{p}_k, \boldsymbol{k}) = \boldsymbol{d}(\boldsymbol{j}_k + \boldsymbol{x}, \boldsymbol{k}) = \boldsymbol{d}(\boldsymbol{j}_k, \boldsymbol{k}) \exp(2\pi \mathrm{i} \boldsymbol{k} \cdot \boldsymbol{x}), \tag{20}$$

where i represent the complex number $\mathrm{i}^2 = -1$. Therefore, consider the nearest unit cell, the displacements of all the dependent joints can be expressed by the displacements of the independent nodes:

$$\boldsymbol{d}(\boldsymbol{j}_k + \hat{\boldsymbol{x}}_k, \boldsymbol{k}) = \mathrm{z}(\boldsymbol{k}, \hat{\boldsymbol{x}}_k) \boldsymbol{d}(\boldsymbol{j}_k, \boldsymbol{k}), \tag{21}$$

where $\mathrm{z}(\boldsymbol{k}, \hat{\boldsymbol{x}}_k) = \exp(2\pi \mathrm{i} \boldsymbol{k} \cdot \hat{\boldsymbol{x}}_k)$, $\hat{\boldsymbol{x}} = \hat{x}_i \boldsymbol{a}_i$, $\hat{x}_i \in \{-1, 0, 1\}$. Then substituting Eq. (21) into Eq. (13) then we obtained:

$$\bar{\boldsymbol{B}}(\boldsymbol{k}) \cdot \bar{\boldsymbol{d}}(\boldsymbol{k}) = \bar{\boldsymbol{e}}(\boldsymbol{k}). \tag{22}$$

Finally, the dynamical matrix of the periodic structure is determined as

$$D(k) = \frac{1}{m} \bar{B}^{\dagger}(k) k_b \bar{B}(k), \tag{23}$$

and the dispersion relation of the lattice can then be obtained by solving

$$\boldsymbol{D}(\boldsymbol{k}) \cdot \bar{\boldsymbol{d}}(\boldsymbol{k}) = \omega^2 \bar{\boldsymbol{d}}(\boldsymbol{k}). \tag{24}$$

The dispersion surfaces of the constructed discrete QM lattice as shown in Fig. 4(b) is exactly the same as the homogeneous QM material as shown in Fig. 1, which are obtained by solving the eigenvalue problem of Eq. (24). Only a little discrepancy regarding to Fig. 1(d) and (f) of polarization at the position where the two modes are tangent, the reason may come from nonzero small quantities appeared at off diagonal places of the elastic matrix (as shown in Eq. (12)).

4. Function design with quadramode material

As discussed in the previous section, if a plane wave is generated on the crystal plane (001) of the QM material, the particle polarization is always perpendicular to this plane, as shown in Fig. 5(a) (also Fig. 1(d) or (f)). The corresponding unit cell and lattice are shown respectively in Fig. 5 (b) and (c). In this section, we will explore this unique property of the QM material to design an out-of-plane shear (SH) polarizer. This SH polarizer is expected to be able to block incoming waterborne sound particularly at low frequency. The principle of this polarizer is illustrated by Fig. 5 (d). When a general polarized wave defined by spherical coordinate components θ and φ is propagating along the x-axis from the left into the QM material, only the part of the incident wave polarized along the z-axis can be transmitted to the right medium, since the QM material at this position can only transmit the shear wave with the polarization as shown by the green double arrows in Fig. 5(d).

A commercially available finite element analysis (FEA) software, COMSOL Multiphysics 5.4, was used for all analysis in the following numerical simulations. Fig. 6 shows the computed refraction

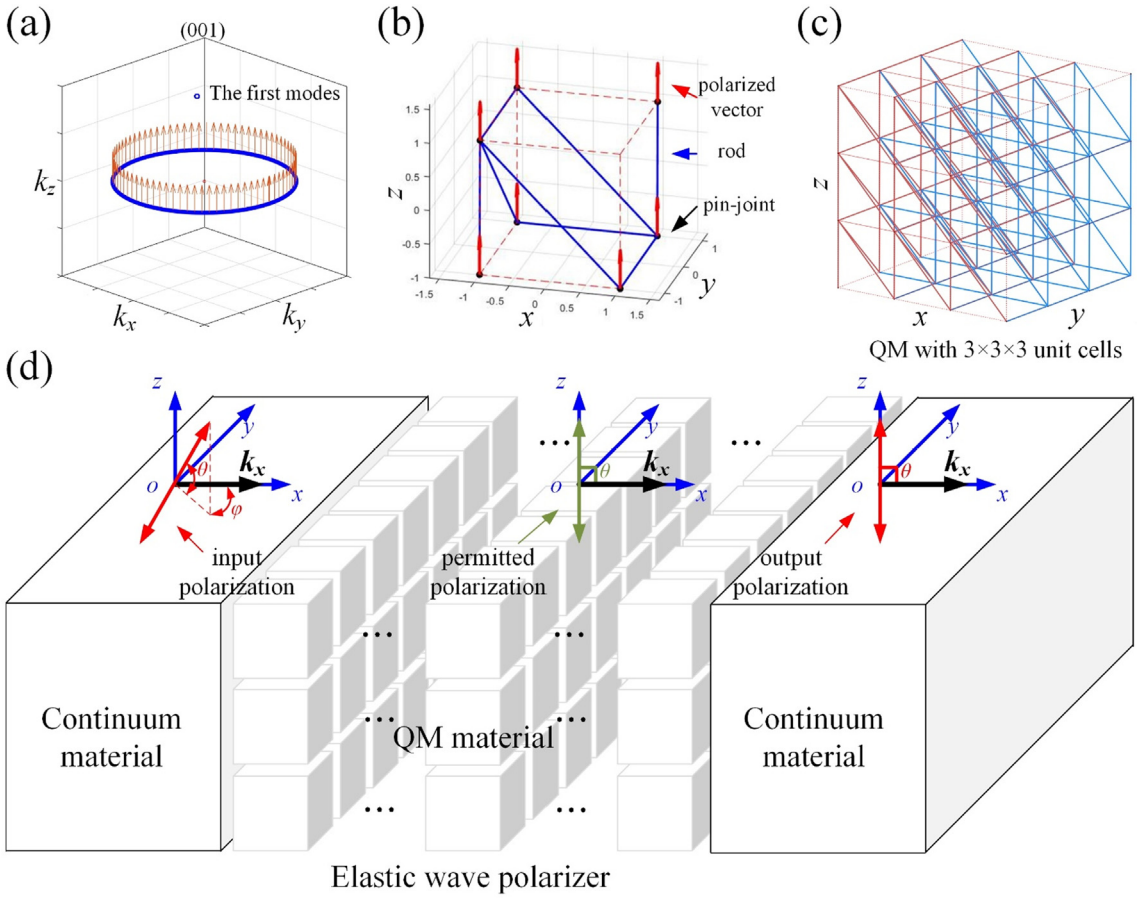

Fig. 5. Illustration of QM metamaterial on wave control. (a) the IFC on (001) and its polarization: blue line and orange arrows respectively; (b) the unit cell of the QM lattice and polarization of wave vectors in any direction on (001); (c) QM material lattice with 3 × 3 × 3 unit cells; (d) principle of SH wave polarizer by using the QM material.

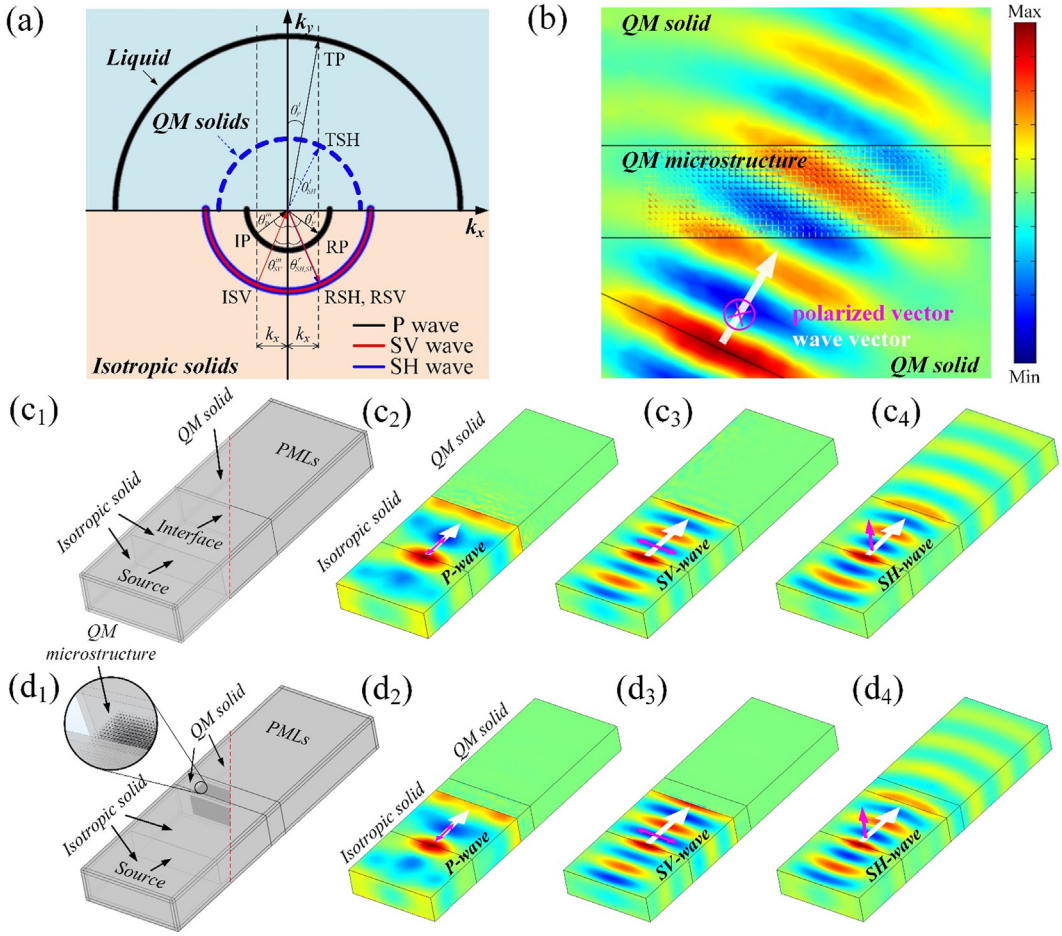

Fig. 6. (a) The IFC on (001) of isotropic solid (bottom) and QM material (top); (b) out-of-plane displacement field, perfect transmission of an SH-wave Gaussian beam incident on a QM lattice from its effective homogeneous counterpart; (c) wave propagation for a normally incident wave initiated from an isotropic solid to the homogenous QM material, c_2, c_3 and c_4 for P-, SV- and SH-wave respectively (the fields are normalized by the incident wave). (d) Same as (c) but the homogeneous QM materials is replaced by its discrete QM lattice.

and reflection at interfaces between the homogenized/discrete QM lattice as well as an isotropic solid, respectively. The dispersion curves of the two semi-infinite homogeneous materials are illustrated in Fig. 6(a) with the following material constants: the isotropic solid (bottom) with elastic constants C_{11}^{ISO} = 105.2GPa, C_{12}^{ISO} = 26.7GPa, density ρ^{ISO} = 2700 kg/m^3 (aluminum), and the QM material (top) with elastic constants $C_{44}^{QM} = C_{55}^{QM}$ = 26.7GPa, density ρ^{QM} = 2000 kg/m^3. We see that there would be three types of wave in the isotropic solid: the reflected P-, SV- and SH-wave (corresponding to RP, RSV and RSH in Fig. 6(a) respectively), and only one type of wave in the QM material: the transmitted SH-wave (TSH). In order to check our designed QM lattice, we examine the wave transmission for a Gaussian SH-wave beam ($\theta_{SH}^{in} = 25^{\circ}$ and with a central frequency f = 50 kHz) incident on a QM lattice (with 15 × 50 × 15 unit cells, 15 layers in thickness direction) from its effective homogeneous counterpart, a perfect transmission is observed as shown in Fig. 6(b), which in fact confirms our design method for the QM material. The unit cell is a cube with a side length of 2 mm. Then the total size of the lattice is 30 mm × 100 mm × 30 mm. Because the homogeneous QM material is a kind of linear Cauchy elastic materials, the perfectly matched layers (PMLs) of Solid Mechanics Module in COMSOL Multiphysics software still work. In the simulation, the computed regions are covered by the PMLs to avoid reflectance due to the finite boundary.

In order to demonstrate the idea to make a SH polarizer with the QM material, we perform numerical simulations on wave propagation for a normally incident Gaussian beam initiated from an isotropic solid to the homogenous or lattice QM materials, different types of wave are considered, including P-wave, SV-wave and SH-wave, the wave propagations represented by the normalized P-, SV- and SH-wave fields are provided by Fig. 6(c) and (d). It should be noted that, in order to show more clearly the characteristics of wave propagation in our 3D QM material, the PMLs were set to be invisible and only the middle part was retained. Clearly, the designed QM material (homogeneous or lattice) blocks both P and SV waves, only SH-wave is allowed to pass through. This effect is similar to that of polarized sunglasses, and can be considered as a 'polarized glass' for elastic waves.

As well-known that liquids support only P wave, if we can design a material which can polarize incoming wave into SH wave, there will not have mode conversion at the interface between this material and the liquid, therefore the incoming wave is not able to transmit into the liquid and will be blocked. To demonstrate this idea, we examine a QM layer sandwiched by an isotropic solid and water, the QM layer acts as a SH wave polarizer. A line source to generate different types of waves (P- and SV-wave) is located in the isotropic solid. The P- and SV- Gaussian beam with a frequency 50 kHz are generated respectively. The material constants of the isotropic material and QM material are the same as in the previous example, and C_{11}^{liquid} = 2.25GPa and ρ^{liquid} = 1000 kg/m^3 for the liquid (water). Fig. 7 shows clearly that with the QM material layer both incoming P- and SV-waves (Fig. 7(b) and (d), respectively) are

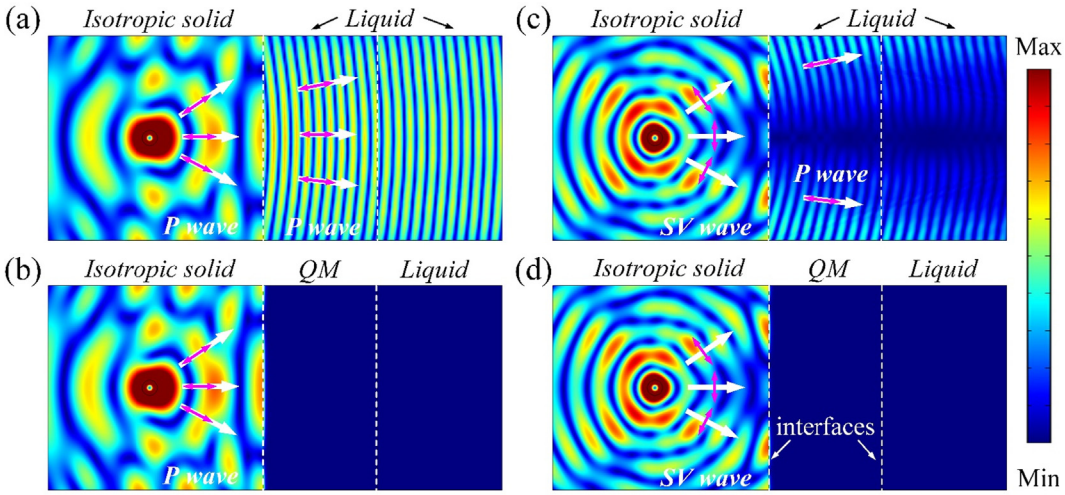

Fig. 7. Displacement field, colors indicate displacement magnitude $|\mathbf{u}| = (u^2 + v^2)^{1/2}$. P wave incident into liquid without (a) and with QM interlayer (b); (c) and (d) Same as (a) and (b) but the incident P wave is replaced by incident SV wave.

stopped, contrary to the cases without the QM layer (Fig. 7(a) and (c), respectively) where mode conversion at the interface allows wave to transmit into water. Fig. 6(a) also shows the IFC and the supported wave in the isotropic solids (bottom), QM layer (top with blue dashed line) and liquid (top with black solid line). In the QM layer, the only supported wave is of SH mode, at the interface between the QM material and water, SH wave is not able to be converted into P or SV waves so it is blocked. Contrary to the QM material, a tradition isotropic solid can convert SV wave to P wave at the interface between water, high transmission is observed as shown in Fig. 7 (c). The shadow along the direction of the normal incidence of SV wave is due to the zero displacement in wave direction. The great advantage of above method is that it can function for a broad frequency band, since only static material property is utilized without resonant mechanism.

5. Conclusions

We have examined systematically a kind of extremal materials, quadramode materials, which elastic matrix has only two no vanishing eigenvalues. The wave properties of some typical QM materials with different material symmetries have been investigated. It is found that QM materials cannot be isotropic, and the number of IFC of QM materials is shown to be less than 2 in agreement of the simulation. The presence of mechanisms or soft modes in this type of materials renders a vast variation of the shape of IFC, offers also unparalleled capacity to control elastic wave. A SH wave polarizer with the QM material is constructed and its application to isolate broadband low frequency waterborne sound is also demonstrated numerically. A corresponding truss model of the QM material supporting any combination of two independent shear stresses is also forwarded, its effective modulus and IFC are compared quite well with the homogenized model. This work provides first systematic study on quadramode material and offer a new possibility to control low frequency elastic wave.

Declaration of Competing Interest

The authors declare that they have no known competing financial interests or personal relationships that could have appeared to influence the work reported in this paper.

Acknowledgments

We thank the support of National Natural Science Foundation of China (Grants No. 11632003, No. 11972083, No. 11991030), and Beijing Science and Technology Commission, China (No. Z191100004819003).

References

[1] L.D. Landau, E.M. Lifshitz, J.B. Sykes, W.H. Reid, Theory of elasticity: Vol. 7 of Course of Theoretical Physics, Pergamon, Oxford, 1986, pp. xv + 35 (ISBN: 0-08-033916-6).
[2] N. Fang, D. Xi, J. Xu, M. Ambati, W. Srituravanich, C. Sun, X. Zhang, Ultrasonic metamaterials with negative modulus, Nat. Mater. 5 (2006) 452–456.
[3] X.N. Liu, G.K. Hu, G.L. Huang, C.T. Sun, An elastic metamaterial with simultaneously negative mass density and bulk modulus, Appl. Phys. Lett. 98 (2011) 251907.
[4] R. Zhu, X.N. Liu, G.K. Hu, C.T. Sun, G.L. Huang, Negative refraction of elastic waves at the deep-subwavelength scale in a single-phase metamaterial, Nat. Commun. 5 (2014) 5510.
[5] H. Nassar, Y.Y. Chen, G.L. Huang, A degenerate polar lattice for cloaking in full two-dimensional elastodynamics and statics, Proc. R. Soc. A Math. Phys. Eng. Sci. 474 (2018) 20180523.
[6] H. Nassar, Y.Y. Chen, G.L. Huang, Isotropic polar solids for conformal transformation elasticity and cloaking, J. Mech. Phys. Solids. 129 (2019) 229–243.
[7] H.K. Zhang, Y. Chen, X.N. Liu, G.K. Hu, An asymmetric elastic metamaterial model for elastic wave cloaking, J. Mech. Phys. Solids. 135 (2020) 103796.
[8] C. Scheibner, A. Souslov, D. Banerjee, P. Surówka, W.T.M. Irvine, V. Vitelli, Odd elasticity, Nat. Phys. 16 (4) (2020) 475–480.
[9] G.W. Milton, A.V. Cherkaev, Which elasticity tensors are realizable?, J Eng. Mater. Technol. ASME. 117 (1995) 483–493.
[10] G.W. Milton, The Theory of Composites, Cambridge University Press, Cambridge, United Kingdom, 2002, pp. xxviii + 719. (ISBN: 0-521-78125-6 (LCCNTA418.9.C6M58 2001)).
[11] M. Kadic, T. Bückmann, N. Stenger, M. Thiel, M. Wegener, On the practicability of pentamode mechanical metamaterials, Appl. Phys. Lett 100 (19) (2012) 191901, https://doi.org/10.1063/1.4709436.
[12] Y. Chen, X.N. Liu, G.K. Hu, Latticed pentamode acoustic cloak, Sci. Rep.-UK 5 (2015) 15745.
[13] Y. Chen, M.Y. Zheng, X.N. Liu, Y.F. Bi, Z.Y. Sun, P. Xiang, J. Yang, G.K. Hu, Broadband solid cloak for underwater acoustics, Phys. Rev. B. 95 (2017) 180104(R).
[14] A.N. Norris, Acoustic cloaking theory, Proc. R. Soc. A. 464 (2008) 2411–2434.
[15] C.N. Layman, C.J. Naify, T.P. Martin, D.C. Calvo, G.J. Orris, Highly Anisotropic Elements for Acoustic Pentamode Application, Phys. Rev. Lett. 111 (2013) 024302.
[16] A.N. Norris, Mechanics of elastic networks, Proc. R. Soc. A. 470 (2172) (2014) 20140522, https://doi.org/10.1098/rspa.2014.0522.
[17] Y. Cheng, X.M. Zhou, G.K. Hu, Broadband dual-anisotropic solid metamaterials, Sci. Rep.-UK 7 (2017) 13197.
[18] H.W. Dong, S.D. Zhao, X.B. Miao, C. Shen, X.D. Zhang, Z.G. Zhao, C.Z. Zhang, Y.S. Wang, L. Cheng, Customized broadband pentamode metamaterials by topology optimization, J. Mech. Phys. Solids. 152 (2021) 104407.

[19] Z.Y. Li, Z. Luo, L.C. Zhang, C.H. Wang, Topological design of pentamode lattice metamaterials using a ground structure method, Mater. Design. 202 (2021) 109523.
[20] T. Bückmann, M. Thiel, M. Kadic, R. Schittny, M. Wegener, An elasto-mechanical unfeelability cloak made of pentamode metamaterials, Nat. Commun. 5 (2014) 4130.
[21] M.Y. Zheng, C.I. Park, X.N. Liu, R. Zhu, G.K. Hu, Y.Y. Kim, Non-resonant metasurface for broadband elastic wave mode splitting, Appl. Phys. Lett. 116 (2020) 171903.
[22] F. Fraternali, A. Amendola, Mechanical modeling of innovative metamaterials alternating pentamode lattices and confinement plates, J. Mech. Phys. Solids. 99 (2017) 259–271.
[23] U.D. Larsen, O. Sigmund, S. Bouwstra, Design and fabrication of compliant micro-mechanisms and structures with negative Poisson's ratio, J. Microelectromech. Syst. 6 (1997) 99–106.
[24] J.N. Grima, K.E. Evans, Auxetic behavior from rotating squares, J. Mater. Sci. Lett. 19 (2000) 1563–1565.
[25] G.W. Milton, Complete characterization of the macroscopic deformations of periodic unimode metamaterials of rigid bars and pivots, J. Mech. Phys. Solids. 61 (7) (2013) 1543–1560.
[26] G.W. Milton, Adaptable nonlinear bimode metamaterials using rigid bars, pivots, and actuators, J. Mech. Phys. Solids. 61 (7) (2013) 1561–1568.
[27] J. Achenbach, Wave Propagation in Elastic Solid, Elsevier, 2012.
[28] J.C. Maxwell, On the calculation of the equilibrium and stiffness of frames, Philos. Mag. 27 (1864), 294–299 (Paper XXVI in Collected papers, Cambridge 1890).
[29] C.R. Calladine, Buckminster Fuller tensegrity structures and Clerk Maxwell rules for the construction of stiff frames, Int. J. Solids. Struct. 14 (1978) 161–172.
[30] T.C. Lubensky, C.L. Kane, X.M. Mao, A. Souslov, K. Sun, Phonons and elasticity in critically coordinated lattices, Rep. Prog. Phys. 78 (2015) 073901.
[31] R.G. Hutchinson, N.A. Fleck, The structural performance of the periodic truss, J. Mech. Phys. Solids. 54 (2006) 756–782.
[32] S.H. Jo, Y.W. Xia, A.G. Moura, H.J. Yoon, Y.C. Shin, A. Erturk, B.D. Youn, Experimentally validated broadband self-collimation of elastic waves, Int. J. Mech. Sci. 192 (2021) 106131.
[33] H.K. Zhang, Z. Kang, Y.Q. Wang, W.J. Wu, Isotropic "Quasi-Fluid" Metamaterials Designed by Topology Optimization, Adv. Theor. Simul. 3 (2020) 1900182.
[34] R. Schittny, T. Bückmann, M. Kadic, M. Wegener, Elastic measurements on macroscopic three-dimensional pentamode metamaterials, Appl. Phys. Lett. 103 (23) (2013) 231905, https://doi.org/10.1063/1.4838663.
[35] A. Martin, M. Kadic, R. Schittny, T. Bückmann, M. Wegener, Phonon band structures of three-dimensional pentamode metamaterials, Phys. Rev. B. 86 (2012) 155116.
[36] S.D. Guest, J.W. Hutchinson, On the determinacy of repetitive structures, J. Mech. Phys. Solids. 51 (2003) 383–391.
[37] A. Souslov, A.J. Liu, T.C. Lubensky, Elasticity and response in nearly isostatic periodic lattices, Phys. Rev. Lett. 103 (2009) 205503.
[38] S. Pellegrino, Structural computations with the singular value decomposition of the equilibrium matrix, Int. J. Solids. Struct. 30 (21) (1993) 3025–3035.
[39] S. Pellegrino, C.R. Calladine, Matrix analysis of statically and kinematically indeterminate frameworks, Int. J. Solids. Struct. 22 (4) (1986) 409–428.